CHIN. PHYS. LETT. Vol. 38, No. 3 (2021) 030303 **Express Letter**

Experimental Protection of the Spin Coherence of a Molecular Qubit Exceeding a Millisecond

Yingqiu Dai(代映秋)[1,2,3†], Yue Fu(伏月)[1,2,3†], Zhifu Shi(石致富)[1,2,3], Xi Qin(秦熙)[1,2,3], Shiwei Mu(穆世伟)[1,2,3], Yang Wu(伍旸)[1,2,3], Ji-Hu Su(苏吉虎)[1,2,3], Yi-Fei Deng(邓义飞)[4], Lei Qin(秦雷)[4], Yuan-Qi Zhai(翟沅琦)[4], Yan-Zhen Zheng(郑彦臻)[4], Xing Rong(荣星)[1,2,3*], and Jiangfeng Du(杜江峰)[1,2,3*]

[1]*Hefei National Laboratory for Physical Sciences at the Microscale and Department of Modern Physics, University of Science and Technology of China, Hefei 230026, China*
[2]*CAS Key Laboratory of Microscale Magnetic Resonance, University of Science and Technology of China, Hefei 230026, China*
[3]*Synergetic Innovation Center of Quantum Information and Quantum Physics, University of Science and Technology of China, Hefei 230026, China*
[4]*Frontier Institute of Science and Technology (FIST), Xi'an Jiaotong University, Xi'an 710054, China*

(Received 31 December 2020; accepted 27 January 2021; published online 6 February 2021)

Molecular qubits are promising as they can benefit from tailoring and versatile design of chemistry. It is essential to reduce the decoherence of molecular qubits caused by their interactions with the environment. Herein the dynamical decoupling (DD) technique is utilized to combat such decoherence. The coherence time for a transition-metal complex $(PPh_4)_2[Cu(mnt)_2]$ is prolonged from 6.8 μs to 1.4 ms. The ratio of the coherence time and the length of $\pi/2$ pulse, defined as the single qubit figure of merit (Q_M), reaches 1.4×10^5, which is 40 times greater than what previously reported for this molecule. Our results show that molecular qubits, with milliseconds coherence time, are promising candidates for quantum information processing.

DOI: 10.1088/0256-307X/38/3/030303

Quantum computation provides great speedup over its classical counterpart for a variety of computational problems.[1] There have been several candidates,[2] including superconductor circuits,[3] trapped ions,[4] defects in solids[5] and quantum dots.[6] More recently, electron spins in magnetic molecule, termed molecular qubits, have been stimulating great interest.[7–25] Compared with other physical systems, molecular qubits have several advantages as the basic building block of quantum computations:[8,25] their structure can be easily tuned by chemical methods, a scalable amount of identical molecular qubits can be routinely produced[26] and deposited in regular arrays on surfaces for addressing.[27] The size of molecular qubit is usually of nanometers, which is suitable for local manipulation and detection[28–30] and is vital for future scalable architecture. Due to the interaction with the local environment, the quantum coherence of the qubit states deteriorates. This remains one of the major obstacles to practical quantum computation based on molecular qubits.

Recently, several approaches have been developed to overcome decoherence of molecular qubits. An efficient method is to dilute the molecular qubits in a diamagnetic matrix[10,11,31,32] and to enhance the conformation rigidity of the molecule.[13–16,33] An alternative approach is to design a nuclear spin free environment by synthesizing the chemical complex.[33,34] This approach restricts the ligand selection and designs to ligands with zero nuclear magnetic dipole moment. It means that the nuclear spins in the environment cannot be used as the resources of quantum computation. Another approach is to use the atomic clock transitions, where the decoherence can be suppressed.[35,36] The longest coherence time of molecular qubits reported thus far is still below one millisecond.[34] Alternatively, the dynamical decoupling (DD) technique can be an effective method to fight against decoherence by averaging the noise.[37,38] This method is not subject to the limitation of molecular synthesis, e.g., replacement of hydrogen with deuterium.[33] Furthermore, DD, which has been used in quantum dots,[39] trapped ions,[40] NV centers[41] and other quantum systems, is compatible with quantum gates by adopting dephasing suppressed quantum control over qubits.[42,43]

In this Letter, we report a molecular qubit's coherence time over one millisecond (1.4 ms) which is prolonged by applying the DD technique. This is among

Supported by the National Key R&D Program of China (Grant Nos. 2018YFA0306600 and 2016YFB0501603), the Chinese Academy of Sciences (Grant Nos. GJJSTD20170001, QYZDY-SSW-SLH004, and QYZDB-SSW-SLH005), and Anhui Initiative in Quantum Information Technologies (Grant No. AHY050000). X.R. thanks the Youth Innovation Promotion Association of Chinese Academy of Sciences for their support. Y.Z.Z. thanks the support from Wuhan National High Magnetic Field Center (Grant No. 2015KF06).
†These authors contributed equally to this work.
*Corresponding authors. Email: xrong@ustc.edu.cn; djf@ustc.edu.cn
© 2021 Chinese Physical Society and IOP Publishing Ltd

the best ones reported so far for magnetic molecular qubits, and the ratio of the coherence time and the length of $\pi/2$ pulse, defined as the single qubit figure of merit ($Q_{\rm M}$), reaches 1.4×10^5. Compared with the method of removing the nuclear spins, the DD technique does not require a special synthesis of the molecule. This makes it possible to further use nuclear spins as qubits. Our result shows that molecular qubits have great potential for quantum computation.

In our experiment, the molecular qubit is composed of a type of transition-metal complexes, $(PPh_4)_2[Cu(mnt)_2]$ (1Cu, mnt^{2-} = maleonitriledithiolate) doped into the diamagnetic isostructural host $(PPh_4)_2[Ni(mnt)_2]$ (1Ni). The compounds 1Cu and 1Ni were prepared according to a literature procedure,[33] and were characterized by x-ray crystallography (see Section 1 in the Supplementary Material for details). The sample was diluted in the diamagnetic isostructural host 1Ni with concentration 0.3%. A home-built X-band pulsed EPR spectrometer[44] was used to measure the prolonged coherence time. The structure of 1Cu is plotted in Fig. 1(a). There is an electron spin which couples with the nearby copper nuclear spin. The corresponding Hamiltonian can be written as $H=\boldsymbol{S}\cdot\boldsymbol{A}\cdot\boldsymbol{I}+\beta_{\rm e}\boldsymbol{B}_0\cdot\boldsymbol{g}_{\rm e}\cdot\boldsymbol{S}-\beta_{\rm n}g_{\rm n}\boldsymbol{B}_0\cdot\boldsymbol{I}$, where $\boldsymbol{S}$ ($\boldsymbol{I}$) stands for the electron (nuclear) spin vector operator, $\beta_{\rm e}$ ($\beta_{\rm n}$) represents the Bohr magneton (nuclear magneton), $\boldsymbol{g}_{\rm e}$ is g tensor of the electron spin, $g_{\rm n}$ is nuclear g factor, $\boldsymbol{B}_0$ is the external magnetic field, and $\boldsymbol{A}$ stands for the hyperfine coupling between the electron and nuclear spins.

Figure 1(b) shows the electron spin resonance spectrum of 1Cu measured by the field sweep electron spin echo detection (FSED) method at temperature 77 K. Blue and red lines are experimental and simulation data, respectively. This spectral shape is due to the anisotropic hyperfine coupling of the electron spin to the $I=3/2$ copper nuclear spin. Spectral fitting yields $g_{\parallel}=2.0898$, $g_{\perp}=2.0215$, $A_{\parallel}=495.4$ MHz and $A_{\perp}=118$ MHz (see Section 2 in the Supplementary Material for details), which are comparable to the reported data.[33] The temperature dependences of relaxation time T_1 (spin-lattice relaxation time) and T_2 (coherence time measured by Hahn echo) are plotted in Fig. 1(c). Spin-lattice relaxation times T_1 were measured from 8 K to 77 K (see Section 3 in the Supplementary Material for details). As the temperature decreases, T_1 increases dramatically and reaches 25 ms at 8 K. The relaxation rate $1/T_1$ is found to be dependent strongly on temperature (T), i.e., $\sim T^3$ [red dashed line in Fig. 1(c)]. This T^3 dependence is assigned as a Raman relaxation which is attributed to different vibrational frequencies between local defect and the lattices.[45] The value of T_2 also increases from 5.5 μs at 71 K to 6.8 μs at 8 K, showing a saturation at low temperature (see Section 4 in the Supplementary Material for details). These are consistent with the previous measurements on 1Cu.[33] These experiments were performed with an ELEXSYS E580 (X-band) Bruker spectrometer.

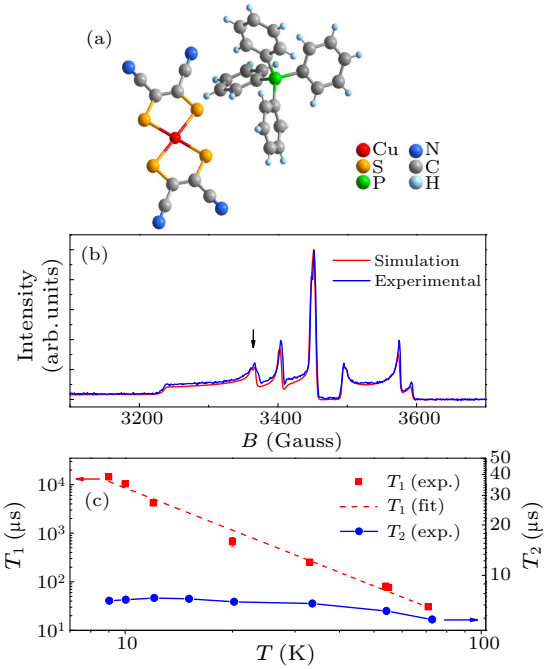

Fig. 1. (a) Structure of 1Cu. Colors: copper-red, sulfur-orange, carbon-grey, nitrogen-blue, phosphorous-green, hydrogen-light blue. (b) Experimental data of FSED spectrum (blue line) and simulations (red line) with parameters of the Hamiltonian in the main text. (c) Temperature dependence of relaxation times T_1 (red squares) and T_2 (blue dots). Red line is fitted according to $1/T_1\propto T^3$. The error bars on the data points are the standard deviations.

Figure 2 shows that the coherence time $T_{\rm coh}$ of this molecular qubit is prolonged by DD sequences at temperature 8 K. The DD sequence is an n-pulse Carr-Purcell-Meiboom-Gill (CMPG-n) sequence with $(\pi/2)_x-\{\tau/2-(\pi)_y-\tau/2\}_n-$echo, where n stands for number of refocusing pulses. The first $(\pi/2)_x$ pulse, which stands for a $\pi/2$ pulse along the x axis in the Bloch sphere, is to generate the quantum coherence. The following $(\pi)_y$ pulses are to invert the state of the electron spin along the y axis in the Bloch sphere periodically, so that the quasi-static external noise (for example, static external magnetic field fluctuations) can be eliminated. When the number of π pulses is fixed, the durations between the pulses τ are varied and then the intensity of echo is recorded. CPMG is a well-accepted method of measuring the coherence time $T_{\rm coh}$, which indicates how long a qubit can remain phase coherent.[1,46] CPMG sequence is robust against pulse errors,[47] which may come from the fluctuation of the microwave field. This robustness allows us to apply up to thousands of π pluses to protect the quantum coherence. The number of refocusing π pulses ranges from 1 to 2048. The spin coherence exhibits a modulated decay behavior as time increases. The decoherence mainly comes from electron spin bath. The coherent oscillations in the signal

are due to the couplings between the molecular qubit and the nearby nuclear spins. The coherence times with CPMG-n, $T_{\rm coh}(n)$, are obtained by fitting the envelopes of echo intensity [red lines in Fig. 2(a)]. The envelope of echo intensity M follows an exponential decay, $M = \exp[-(t/T_{\rm coh})^{\beta}]$, where β is the stretch factor (see Section 5 in the Supplementary Material for details).

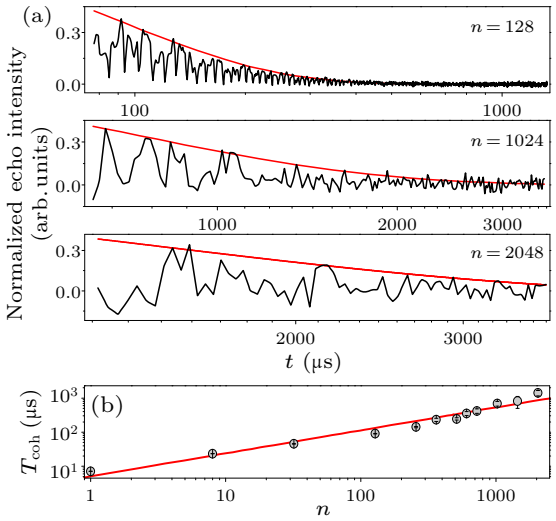

Fig. 2. (a) Echo intensity decay under different CPMG-n pulse sequences with total evolution time, $t = n\tau$. The coherence times with different CPMG sequences are obtained by fitting the envelopes of echo intensity decay (black lines) to $\exp[-(t/T_{\rm coh})^{\beta}]$, where β is the stretch factor. (b) Coherence times (black dots with error bars) under different numbers of π pulses with scaling $T_{\rm coh}(n) \propto n^{0.67}$ (red line). The error bars on the data points are the standard deviations.

Figure 2(b) shows coherence time $T_{\rm coh}$ as a function of DD pulse number n. The coherence time $T_{\rm coh}$ scales as $T_{\rm coh} = T_{2c} \times n^{\alpha}$, where $\alpha = 0.67 \pm 0.04$ is obtained by fitting the data in Fig. 2(b) with T_{2c} being the free fitting parameter. The result gives $T_{2c} = 5.2 \pm 0.4\,\mu$s, which is close to the value with the spin echo measurement (6.8 μs). This scaling is similar to the decoherence behavior due to an electron spin bath, which was discussed in Ref. [41]. Because of the broad FSED spectrum [about 550 Gauss as shown in Fig. 1(b)] and the limited pulse excitation bandwidth (about 100 MHz with a 10 ns $\pi/2$ pulse), about 94% of the electron spins are not excited by the microwave pulses. The off-resonance electron spins behave as an electron spin bath. With 2048 pulses, the coherence time reaches 1.4 ± 0.2 ms, which is 20 times greater than that of the previous work.[33] The improvement of the coherence time is not saturated. Longer coherence time can be expected if more refocusing π pulses are applied. In practice, the performance of DD is limited by the imperfection of the pulses, the minimum time delay between refocusing π pulses and the longitudinal relaxation time. There is also a limitation on the number of the pulses due to the solid-state amplifier in our spectrometer.

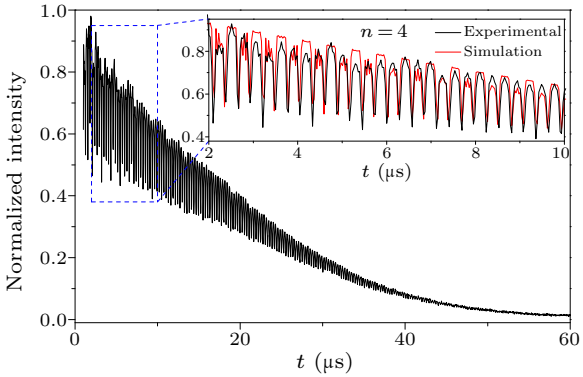

Fig. 3. Echo intensity decay under CPMG-4 pulse sequences with total evolution time $t = 4\tau$. Dips of modulation in coherence decay are mainly induced by ^{1}H nuclear spins. The simulation (red line) with effect of ^{1}H nuclear spins is according with the experimental result (black line).

Moreover, the coherence under different CPMG sequences provides fruitful information about the environment. The modulation in coherence decay comes from the hyperfine couplings between the molecular qubit and the nearby nuclear spins. A model to explain this coherence phenomenon is that the behavior of incoherent nuclear spins around center electron spins could be taken as randomly generated AC magnetic fields.[48] When DD is applied to the molecular qubits, the AC magnetic field will lead to the coherence dips of electron spins at time $t_{\rm dip} = (2k - 1)n/2f_{\rm L}$, where k is dip order and $f_{\rm L}$ is Larmor frequency of nearby nuclear spins. In our experiment, dips are mainly induced by ^{1}H nuclear spins (see Section 5 in the Supplementary Material for details). The experimental observation is in line with the theoretical analysis shown in Ref. [49]. In order to quantify the modulation in coherence decay, we performed numerical calculation. The calculation was carried out by considering the filter function of the CPMG sequence and a Gaussian function for the noise spectral density of the ^{1}H nuclear spin bath.[50] Figure 3 shows that the experimental result is in very good agreement with the simulated one. When more than 1000 DD pulses are applied on the electron spin, negative spin coherence is observed as shown in Fig. 2(a). This phenomenon can be explained by a quantum mechanism which treats the environmental nuclear spins as another quantum system (see Section 5 in the Supplementary Material for details). If the coherence time is prolonged by DD to about several hundreds of microseconds, the effect of the evolution of the nuclear spins cannot be ignored anymore. Spin coherence can be expressed by $L(t) = \langle J_0(t)|J_1(t)\rangle$, where $|J_0(t)\rangle$ and $|J_1(t)\rangle$ are nuclear spin states corresponding to electron spin states $|m_S = 1/2\rangle$ and $|m_S = -1/2\rangle$ at time t, respectively. In this quantum decoherence picture, the spin coherence is bounded between -1 and 1.[48,51]

In order to give the upper bound of the extended coherence by DD, we performed the spin-locking

experiment.[52] The decay time constant achieved by spin-locking is rotation frame relaxation time, $T_{1\rho}$, which is the upper bound of the coherence time prolonged by DD and characterizes the isolation between a spin qubit and the environment.[46] Figure 4 shows the experimental $T_{1\rho}$ under different strengths of the microwave field, ω_1. Inset of Fig. 4(a) shows the pulse sequence for $T_{1\rho}$ measurement. The electron spin is first prepared to a coherent state by a $\pi/2$ pulse around the y axis, and the following microwave pulse with duration $\tau_{\rm p}$ is applied to drive the spin vector rotating around the x axis. After the duration τ_0, a refocusing π pulse is applied for echo detection. As shown in Fig. 4(a), $T_{1\rho}$ with $\omega_1 = 3.96$ MHz is 1.07(3) ms. When the strength of the microwave is enhanced, the value of $T_{1\rho}$ can be extended towards T_1.[53] Figure 4(b) shows that $T_{1\rho}$ can be prolonged by increasing the strength of the microwave field. Since the long microwave pulse with microwave field higher than 4 MHz will destroy the microwave limiter before the low noise amplifier in our setup, measurements with higher microwave power were not carried out. In the future, when a more robust microwave limiter is installed, longer $T_{1\rho}$ can be expected when the strength of the microwave field increases.

It is desirable to compare the molecular qubit with other typical physical systems for quantum computation.[54] This is summarized in Table 1. Macroscopic systems, such as superconducting circuit (SC) qubits with micrometer size, provide good tunability, scalability, flexibility and strong coupling to external fields. The coherence time of SC qubit is relatively short. Recent reported coherence time of SC qubit is about ∼85 μs.[55] The single qubit figure of merit of SC qubit is about 8.5×10^4 with 1 ns typical operation time. On the other hand, microscopic systems, such as spins[56,57] and atoms[58] with atomic scale, can be utilized as qubits with relatively long coherence time. However, the scalability is very challenging for these microscopic systems. Molecular qubits, with the high capacity to form non-trivial ordered states at the nanoscale,[25] are very attractive for future scalability.[28–30] Now, using DD, we are able to enhance the coherence time of a molecular qubit longer than one millisecond.

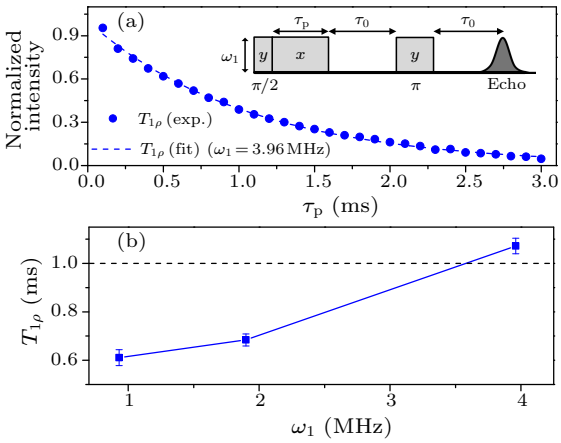

Fig. 4. (a) $T_{1\rho}$ is measured to be 1.07(3) ms (blue dots) when $\omega_1 = 3.96$ MHz. The blue dashed line is the exponential decay fit of the experimental data. Inset shows the pulse sequence of the $T_{1\rho}$ measurement. (b) $T_{1\rho}$ as a function of applied Rabi frequency ω_1. $T_{1\rho}$ is extended when ω_1 is enhanced. The error bars on the data points are the standard deviations.

Table 1. Comparison between different systems used as qubits.

Systems	Typical singe-qubit gate operating time	Coherence time $T_{\rm coh}$	$Q_{\rm M}$
Superconducting qubit[55]	1 ns	∼85 μs	8.5×10^4
Phosphorous doped in silicon[56]	1 μs	0.56 s	5×10^5
NV center in diamond[57]	∼10 ns	1.58 s	$\sim1.6\times10^8$
Trapped ion[59]	1–100 μs	5500 s	$\sim10^7$
Molecular qubit (this work)	10 ns	1.4 ms	1.4×10^5

In conclusion, we have reported, for the first time, the prolonging of the coherence time of a molecular qubit to 1.4 ms by DD, which is about twenty folds longer than the 68 μs achieved for the same qubit but in a deuterated environment.[33] It is worth noting that the molecular qubit in our experiment is not isotopic purified. This means that the surrounding nuclear spins may play important roles as additional nuclear spin qubits. The single qubit figure of merit ($Q_{\rm M}$) of 1.4×10^5 is reached, which is far beyond a $Q_{\rm M}$ value of 10000 set by fault tolerant quantum computing.[60] In the future, advanced quantum control[61] can be applied in molecular qubits to perform high-fidelity quantum gates.[62] Furthermore, the universal dynamical decoupling sequence, such as XY (in which π pulses is along X and Y axes alternately) and Knill DD,[63,64] can protect the coherence of the arbitrary initial state. Our work marks an important step towards quantum computation and quantum sensing[65,66] with molecular systems.

We would like to thank C. Duan for helpful discussion.

References

[1] Nielsen M A and Chuang I L 2000 *Quantum Computation and Quantum Information* (New York: Cambridge University Press) p 546
[2] Ladd T D *et al.* 2010 *Nature* **464** 45
[3] Nakamura Y, Pashkin Y A and Tsai J 1999 *Nature* **398** 786
[4] Wineland D J 1998 *J. Res. Natl. Inst. Stand. Technol.* **103**

259
[5] Gruber A *et al.* 1997 *Science* **276** 2012
[6] Loss D and DiVincenzo D P 1998 *Phys. Rev. A* **57** 120
[7] Leuenberger M N and Loss D 2001 *Nature* **410** 789
[8] Gaita-Ariño A *et al.* 2016 *Inorg. Chem. Front.* **3** 568
[9] Ding Y S, Deng Y F and Zheng Y Z 2016 *Magnetochemistry* **2** 40
[10] Nellutla S *et al.* 2007 *Phys. Rev. Lett.* **99** 137601
[11] Atzori M *et al.* 2016 *J. Am. Chem. Soc.* **138** 2154
[12] Timco G A *et al.* 2009 *Nat. Nanotechnol.* **4** 173
[13] Wedge C J *et al.* 2012 *Phys. Rev. Lett.* **108** 107204
[14] Graham M J *et al.* 2014 *J. Am. Chem. Soc.* **136** 7623
[15] Atzori M *et al.* 2016 *J. Am. Chem. Soc.* **138** 11234
[16] Yu C J *et al.* 2016 *J. Am. Chem. Soc.* **138** 14678
[17] Baldoví J J *et al.* 2013 *Chem. Commun.* **49** 8922
[18] Aguila D *et al.* 2014 *J. Am. Chem. Soc.* **136** 14215
[19] Pedersen K S *et al.* 2016 *J. Am. Chem. Soc.* **138** 5801
[20] Bertaina S *et al.* 2008 *Nature* **453** 203
[21] Yang J *et al.* 2012 *Phys. Rev. Lett.* **108** 230501
[22] Morton J J L *et al.* 2005 *Phys. Rev. Lett.* **95** 200501
[23] Jenkins M D *et al.* 2017 *Phys. Rev. B* **95** 064423
[24] Godfrin C *et al.* 2017 *Phys. Rev. Lett.* **119** 187702
[25] Gaita-Ariño A *et al.* 2019 *Nat. Chem.* **11** 301
[26] Moreno-Pineda E *et al.* 2018 *Chem. Soc. Rev.* **47** 501
[27] Barth J V 2007 *Annu. Rev. Phys. Chem.* **58** 375
[28] Vincent R *et al.* 2012 *Nature* **488** 357
[29] Thiele S *et al.* 2014 *Science* **344** 1135
[30] Fernandez A *et al.* 2016 *Nat. Commun.* **7** 10240
[31] Kaminski D *et al.* 2014 *Phys. Rev. B* **90** 184419
[32] Ardavan A *et al.* 2007 *Phys. Rev. Lett.* **98** 057201
[33] Bader K *et al.* 2014 *Nat. Commun.* **5** 5304
[34] Zadrozny J M *et al.* 2015 *ACS Cent. Sci.* **1** 488
[35] Shiddiq M *et al.* 2016 *Nature* **531** 348
[36] Zadrozny J M *et al.* 2017 *J. Am. Chem. Soc.* **139** 7089
[37] Du J *et al.* 2009 *Nature* **461** 1265
[38] Rong X *et al.* 2011 *Sci. Bull.* **56** 591
[39] Medford J *et al.* 2012 *Phys. Rev. Lett.* **108** 086802
[40] Bermudez A *et al.* 2012 *Phys. Rev. A* **85** 040302
[41] Bar-Gill N *et al.* 2012 *Nat. Commun.* **3** 858
[42] Wang X *et al.* 2012 *Nat. Commun.* **3** 997
[43] Rong X *et al.* 2014 *Phys. Rev. Lett.* **112** 050503
[44] Shi Z *et al.* 2018 *Rev. Sci. Instrum.* **89** 125104
[45] Feng P *et al.* 2012 *Phys. Lett. A* **376** 2195
[46] Vandersypen L M K, Chuang I L 2005 *Rev. Mod. Phys.* **76** 1037
[47] Shim J H *et al.* 2012 *Europhys. Lett.* **99** 40004
[48] Zhao N *et al.* 2012 *Nat. Nanotechnol.* **7** 657
[49] Mitrikas G and Prokopiou G 2015 *J. Magn. Reson.* **254** 75
[50] Mitrikas G, Efthimiadou E K and Kordas G 2014 *Phys. Chem. Chem. Phys.* **16** 2378
[51] Reinhard F *et al.* 2012 *Phys. Rev. Lett.* **108** 200402
[52] Naydenov B *et al.* 2011 *Phys. Rev. B* **83** 081201
[53] Johnson B C and Goldburg W I 1966 *Phys. Rev.* **145** 380
[54] Xiang Z L *et al.* 2013 *Rev. Mod. Phys.* **85** 623
[55] Yan F *et al.* 2016 *Nat. Commun.* **7** 12964
[56] Muhonen J T *et al.* 2014 *Nat. Nanotechnol.* **9** 986
[57] Abobeih M H *et al.* 2018 *Nat. Commun.* **9** 2552
[58] Harty T P *et al.* 2014 *Phys. Rev. Lett.* **113** 220501
[59] Wang P *et al.* 2021 *Nat. Commun.* **12** 233
[60] DiVincenzo D P 2000 *Fortschr. Phys.* **48** 771
[61] Rong X *et al.* 2015 *Nat. Commun.* **6** 8748
[62] Ferrando-Soria J *et al.* 2016 *Nat. Commun.* **7** 11377
[63] De Lange G *et al.* 2010 *Science* **330** 60
[64] Souza A M, Alvarez G A, Suter D 2011 *Phys. Rev. Lett.* **106** 240501
[65] Czap G *et al.* 2019 *Science* **364** 670
[66] Verlhac B *et al.* 2019 *Science* **366** 623

Supplementary Material for

Experimental protection of the spin coherence of a molecular qubit exceeding a millisecond

Yingqiu Dai,[1,2,3] Yue Fu,[1,2,3] Zhifu Shi,[1,2,3] Xi Qin,[1,2,3] Shiwei Mu,[1,2,3] Yang Wu,[1,2,3] Ji-Hu Su,[1,2,3] Yi-Fei Deng,[4] Lei Qin,[4] Yuan-Qi Zhai,[4] Yan-Zhen Zheng,[4] Xing Rong,[1,2,3,*] and Jiangfeng Du[1,2,3,†]

[1] *Hefei National Laboratory for Physical Sciences at the Microscale and Department of Modern Physics, University of Science and Technology of China, Hefei 230026, China*
[2] *CAS Key Laboratory of Microscale Magnetic Resonance, University of Science and Technology of China, Hefei 230026, China*
[3] *Synergetic Innovation Center of Quantum Information and Quantum Physics, University of Science and Technology of China, Hefei 230026, China*
[4] *Frontier Institute of Science and Technology (FIST), Xi'an Jiaotong University, Xi'an 710054, China*

I. SAMPLE PREPARATION

We prepared the compounds **1Cu** and **1Ni** according to a literature procedure[1]. Bis- (tetraphenylphosphonium) - bis -(maleonitriledithiolato)cuprate $(PPh_4)_2[Cu(mnt)_2]$ (**1Cu**): Sodium malontriledithiolate (279 mg, 1.5 mmol) was dissolved in 5 ml ethanol and 2 ml demineralized water. Subsequently copper chloride dihydrate (128 mg, 0.75 mmol), dissolved in 5 ml ethanol, and tetraphenylphosphonium bromide (629 mg, 1.50 mmol), dissolved in 15 ml ethanol were added under stirring. The brown product precipitated immediately and was separated from the solution after 5 min by vacuum filtration. Washing of the product with 3×5 ml ethanol and drying for 20 hours under reduced pressure. Bis-(tetraphenylphosphonium)-bis-(maleonitriledithiolato)nickelate $(PPh_4)_2[Ni(mnt)_2]$ (**1Ni**): The same procedure as described for **1Cu** was executed with nickel chloride hexahydrate (178 mg, 0.75 mmol) instead of copper chloride dihydrate. Doped powder: 0.3% of **1Cu** in **1Ni**: Doped powders were obtained by dissolving compounds **1Cu** and **1Ni** in the molar ratio 0.3 : 99.7 in a minimum volume of acetone, which was subsequently evaporated under reduced pressure. The resulting powders were dried in vacuo and finely ground. We characterize the samples by XRD spectroscopy and find that the experimental results are in good agreement with the numerical simulation as shown in the Fig. S1.

II. SIMULATION OF THE FSED

The fitting of the FSED is implemented by EasySpin[2], which is an open-source MATLAB toolbox for simulating Electron Paramagnetic Resonance spectra. We fit the FSED spectrum following the reference[2], yielding $g_{\parallel} = 2.0898$, $g_{\perp} = 2.0215$, $A_{\parallel} = 495.4$ MHz and $A_{\perp} = 118$ MHz.

III. T1 MEASUREMENT

The spin-lattice relaxation times T_1 is measured with inversion recovery method with the sequence $\pi - \tau_1 - \pi/2 - \tau_0 - \pi - \tau_0 - echo$ as shown in the inset of Fig. S2. The length of the π pulse is 48 ns. We show the T_1 measured at 9 K as an example in Fig. S2. The echo intensity follows an exponential relationship, $A_1 \exp[-(t/T_1)^{\beta_1} + B_1]$, where β_1 is the stretch factor. The result gives $T_1 = 14.4(3)$ ms.

* xrong@ustc.edu.cn
† djf@ustc.edu.cn

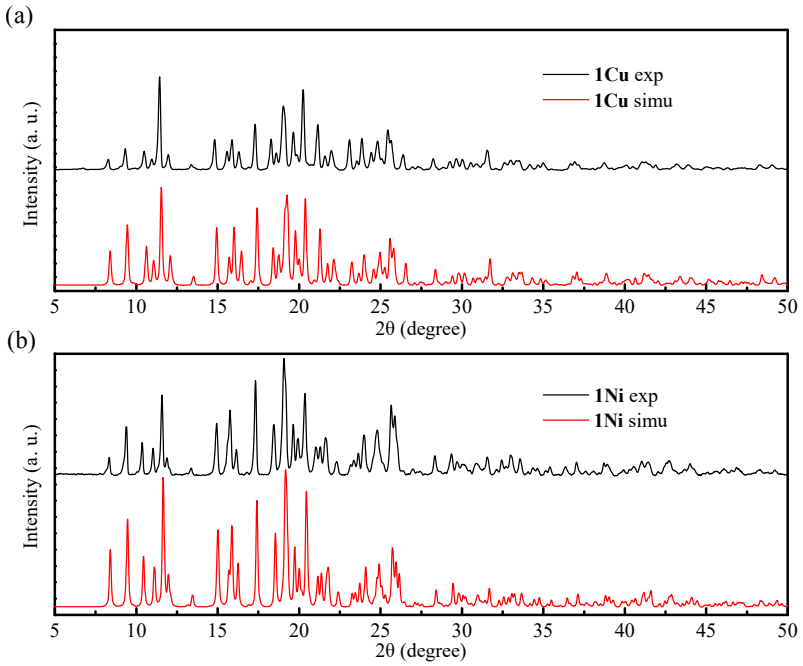

FIG. S1. (Color online). Powder X-ray Diffraction. XRD pattern of (a) **1Cu** and (b) **1Ni**. Black (red) lines denote the experimental (simulated) results.

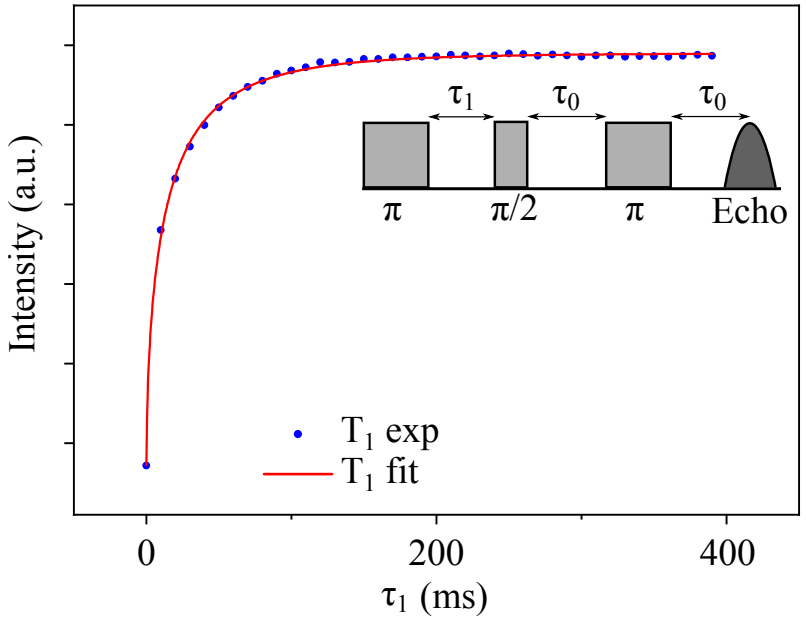

FIG. S2. (color online). T_1 measurement for **1Cu**. T_1 is measured to be 14.4(3) ms (blue dots) at 9 K. The red line is the exponential fitting of the experimental data. Inset shows the pulse sequence of the T_1 measurement.

IV. T2 MEASUREMENT

The T_2 is measured with spin echo sequence $\pi/2 - \tau_2/2 - \pi - \tau_2/2 - echo$ as shown in the inset of Fig. S3. The length of the π pulse is also 48 ns. Fig. S3 shows the T_2 measured at 9 K. The echo intensity follows an exponential decay, $A_2 \exp[-(t/T_2)^{\beta_2} + B_2]$, where β_2 is the stretch factor. The result gives $T_2 = 7.06(4)$ μs.

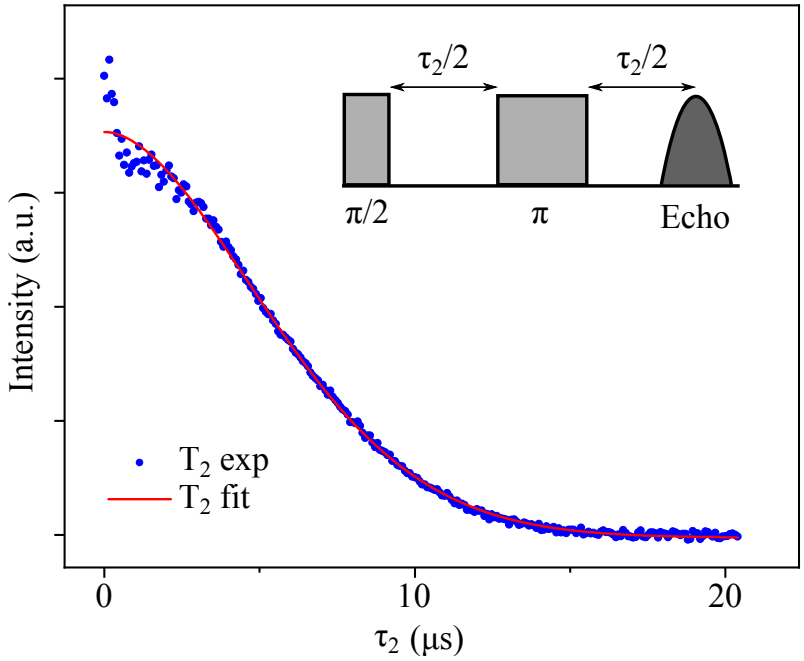

FIG. S3. (color online). T_2 measurement for **1Cu**. T_2 is measured to be 7.06(4) μs (blue dots) at 9 K. The red line is the exponential decay fitting of the experimental data. Inset shows the pulse sequence of the T_2 measurement.

V. SIMULATION OF THE CPMG EXPERIMENTAL RESULTS

The coherence decay of the **1Cu** molecular qubit is described in the general form $C(t) = e^{-\chi(t)}$, where the functional $\chi(t)$ describes the time dependence of the decoherence process[3]. In the present of the pulse sequence on **1Cu** molecular qubit, the decoherence functional is given by

$$\chi(t) = \frac{1}{\pi}\int_0^\infty d\omega S(\omega)\frac{F(\omega t)}{\omega^2}, \tag{1}$$

where the filter function $F(\omega t)$ characterize the pulse sequence in the frequency domain. The filter function of CPMG sequence depend on the number of pulses N and the distribution of π-pulses can be written as[4]

$$F(\omega t) = |1 + (-1)^{N+1}e^{i\omega t} + 2\sum_{j=1}^{N} e^{i\delta_j \omega t}\cos(\omega\tau_\pi/2)|, \tag{2}$$

where $\delta_j \in [0, 1]$ is the normalized position of the centre of the jth π-pulse between the two $\pi/2$-pulses, $t = N\tau$ is the total free-induction time and τ_π is the length of each π-pulse. The simulation of the coherence decay under CPMG experiment is done by treating the nuclear spin bath as the classical noise with a Gaussian noise spectral density coming from different nuclear spins. The total noise spectrum can be written as

$$S(\omega) = \sum_i A_i \exp(-(\omega - \omega_{Li})/2{\sigma_i}^2)/(\sigma_i\sqrt{2\pi}), \tag{3}$$

where $i \in \{\mathrm{H}, \mathrm{C}, \mathrm{P}\}$ corresponding to the molecule composition of **1Cu**. A_i, σ_i and ω_{Li} are the intensity, broadening and center frequency of each nuclear spin noise spectrum. The envelope of echo intensity $C(t)$ follows an exponential decay, $M = \exp[-(t/T_{coh})^\beta]$, where β is the stretch factor. When $N = 1$, the fitting result of β is 1.90. As N increases, β quickly approaches 1. In order to suppress the fitting error of T_{coh}, we lock β to 1 for fitting when $N \geq 8$. The modulation of the spin coherence is fitted by considering the filter function of the CPMG sequence $F(\omega t)$ and the noise spectral density $S(\omega)$. For the case of CPMG-4, the dips in the coherence decay are mainly induced by ^{1}H nuclear spins. There is a peak in the noise spectrum at the frequency 14.33 MHz, which matches the Larmor frequency of ^{1}H. The modulation depth is enhanced with the increasing of the number of π pulses in the CPMG sequence. The weak noise signals of ^{13}C and ^{31}P emerge, yielding two more peaks in the noise spectrum. Fig. S4 shows the simulation

result of 512 pulses. In this case, there are three peaks in the noise spectrum at the frequencies 14.33 MHz, 3.63 MHz and 5.81 MHz, which match the Larmor frequencies of ^{1}H, ^{13}C and ^{31}P, respectively. The simulation result agrees well with the experimental data. When more than 1000 DD pulses are applied, the quantum effect of the nuclear spin bath emerges and the negative spin coherence is observed. While the simulation process discussed above can only be used when the coherence is always positive. So the simulation of the CPMG-4 experiment does not apply to the case of the pulse number larger than 1000.

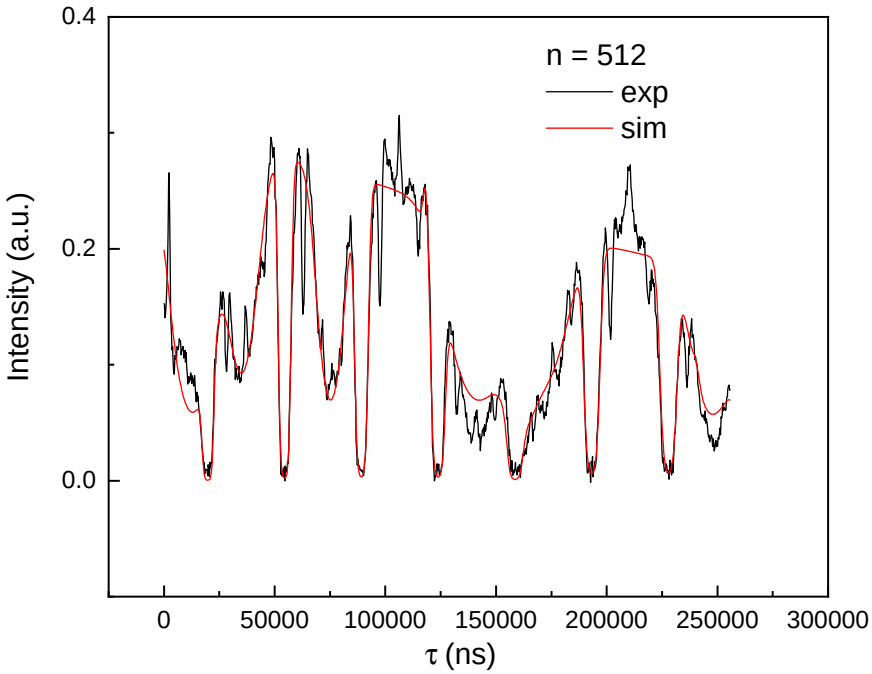

FIG. S4. (color online). Echo intensity decay under CPMG-512 pulse sequences. Dips of modulation in coherence decay are induced by ^{1}H, ^{13}C and ^{31}P nuclear spins. The simulation (red line) with effect of the nuclear spins is according with the experimental result (black line).

[1] Bader, K. *et al.*, *Nat. commun.* **5**, 1-5 (2014).
[2] Stoll, S., Schweiger, A. *J. Magn. Reson.* **178**, 42-55 (2006).
[3] Cywiński, L., Lutchyn, R. M., Nave, C. P. & Das Sarma, S. *Phys. Rev. B* **77**, 174509 (2008).
[4] Biercuk, M. J. *et al.*, *Nature* **458**, 996-1000 (2009).